Received: 9 March 2021 | Revised: 3 June 2021 | Accepted: 8 June 2021

DOI: 10.1002/hbm.25575

RESEARCH ARTICLE

WILEY

Classification of type 2 diabetes mellitus with or without cognitive impairment from healthy controls using high-order functional connectivity

Yuna Chen[1,2] | Zhen Zhou[2] | Yi Liang[3] | Xin Tan[3] | Yifan Li[1] | Chunhong Qin[3] | Yue Feng[1] | Xiaomeng Ma[1] | Zhanhao Mo[2,4] | Jing Xia[5] | Han Zhang[5] | Shijun Qiu[3] | Dinggang Shen[6,7,8]

[1]The First School of Clinical Medicine, Guangzhou University of Chinese Medicine, Guangzhou, Guangdong, China

[2]Department of Radiology and BRIC, University of North Carolina at Chapel Hill, Chapel Hill, North Carolina

[3]Department of Radiology, The First Affiliated Hospital of Guangzhou University of Chinese Medicine, Guangzhou, Guangdong, China

[4]Department of Radiology, China-Japan Union Hospital of Jilin University, Changchun, Jilin, China

[5]Institute of Brain-Intelligence Technology, Zhangjiang Lab, Shanghai, China

[6]School of Biomedical Engineering, ShanghaiTech University, Shanghai, China

[7]Shanghai United Imaging Intelligence Co., Ltd., Shanghai, China

[8]Department of Artificial Intelligence, Korea University, Seoul, Republic of Korea

Correspondence
Han Zhang, Institute of Brain-Intelligence Technology, Zhangjiang Lab, Shanghai 201210, China.
Email: hanzhang.bit@gmail.com

Shijun Qiu, Department of Radiology, The First Affiliated Hospital of Guangzhou University of Chinese Medicine, Guangzhou, Guangdong 510405, China.
Email: qiu-sj@163.com

Dinggang Shen, School of Biomedical Engineering, ShanghaiTech University, Shanghai, China.
Email: dinggang.shen@gmail.com

Funding information
Excellent Doctoral and PhD Thesis Research Papers Project of Guangzhou University of Chinese Medicine, Grant/Award Number: A1-2606-19-429-006; Guangzhou Science and Technology Planning Project, Grant/Award Number: 2018-1002-SF-0442; National Natural Science Foundation of China, Grant/Award Numbers: 81771344, 81920108019, 91649117

Abstract

Type 2 diabetes mellitus (T2DM) is associated with cognitive impairment and may progress to dementia. However, the brain functional mechanism of T2DM-related dementia is still less understood. Recent resting-state functional magnetic resonance imaging functional connectivity (FC) studies have proved its potential value in the study of T2DM with cognitive impairment (T2DM-CI). However, they mainly used a mass-univariate statistical analysis that was not suitable to reveal the altered FC "pattern" in T2DM-CI, due to lower sensitivity. In this study, we proposed to use high-order FC to reveal the abnormal connectomics pattern in T2DM-CI with a multivariate, machine learning-based strategy. We also investigated whether such patterns were different between T2DM-CI and T2DM without cognitive impairment (T2DM-noCI) to better understand T2DM-induced cognitive impairment, on 23 T2DM-CI and 27 T2DM-noCI patients, as well as 50 healthy controls (HCs). We first built the large-scale high-order brain networks based on temporal synchronization of the dynamic FC time series among multiple brain region pairs and then used this information to classify the T2DM-CI (as well as T2DM-noCI) from the matched HC based on support vector machine. Our model achieved an accuracy of 79.17% in T2DM-CI

Yuna Chen and Zhen Zhou share the joint first authorship.

Han Zhang, Shijun Qiu, and Dinggang Shen share the joint senior authorship.

versus HC differentiation, but only 59.62% in T2DM-noCI versus HC classification. We found abnormal high-order FC patterns in T2DM-CI compared to HC, which was different from that in T2DM-noCI. Our study indicates that there could be widespread connectivity alterations underlying the T2DM-induced cognitive impairment. The results help to better understand the changes in the central neural system due to T2DM.

KEYWORDS
cognitive impairment, dynamic functional connectivity, machine learning, resting-state brain networks, type 2 diabetes mellitus

1 | INTRODUCTION

Type 2 diabetes mellitus (T2DM) is a type of complex metabolic disorder characterized by variable degrees of insulin resistance, impaired insulin secretion, and increased glucose production (Kakrani, Gokhale, Vohra, & Chaudhary, 2014). It accounts for 90–95% of diabetes cases and is estimated to affect ~450 million adults globally (Wood et al., 2016), with the number still increasing (Atlas, 2015). Clinical research indicates that T2DM may be associated with accelerated cognitive decline (Biessels, Strachan, Visseren, Kappelle, & Whitmer, 2014; Cheng, Huang, Deng, & Wang, 2012; Geijselaers, Sep, Stehouwer, & Biessels, 2015; Groeneveld et al., 2019), even dementia (Biessels, Staekenborg, Brunner, Brayne, & Scheltens, 2006; Exalto, Whitmer, Kappele, & Biessels, 2012). The comorbidity has a wide spectrum involving various functions, such as motor (Elkayam et al., 2019; Gorniak, Ray, Lee, & Wang, 2020), executive (Redondo, Beltrán-Brotóns, Reales, & Ballesteros, 2016; Vincent & Hall, 2015), psychomotor (Ryan & Geckle, 2000), verbal memory (Messier, 2005), and visual memory (Callisaya et al., 2019). Among the symptoms, cognitive impairments in T2DM could become worse with longer diabetes duration (Gregg et al., 2000) and/or poor glycemic control (Kanaya, Barrett-Connor, Gildengorin, & Yaffe, 2004).

Clinical studies have suggested that factors causing T2DM with cognitive impairment (T2DM-CI) include insulin dysregulation (Verdile, Fuller, & Martins, 2015), hypoglycemia (Marseglia et al., 2016), microvascular diseases (Saedi, Gheini, Faiz, & Arami, 2016), elevated levels of inflammatory cytokines (Meneilly & Tessier, 2016), APOE-epsilon 4 allele (Dore, Elias, Robbins, Elias, & Nagy, 2009), and chronic exposure to high-level glucose (Ghasemi, Haeri, Dargahi, Mohamed, & Ahmadiani, 2013). However, how the brain changes in patients with T2DM-CI is unclear. There are scattered reports using noninvasive structural magnetic resonance imaging (MRI) that revealed the widespread gray matter loss in the medial temporal, anterior cingular, and medial frontal cortices, as well as white matter loss in the frontal and temporal regions, might be associated with T2DM-CI (Moran et al., 2013). Nevertheless, other studies favor the hypothesis that it could be specific to and localized in brain regions, such as hippocampus, that are targeted in T2DM (Brundel et al., 2010; den Heijer et al., 2003). Studies also found that the impaired executive and memory functions might be related to the decreased gray matter density and reduced glucose metabolism in the orbital prefrontal, temporal, and cerebellar regions (Garcia-Casares et al., 2014), further linking the general clinical etiology with brain structural and functional alterations (Cheng, Liu, Zhang, Munsell, & Shen, 2015; Fan et al., 2007). In recent years, resting-state functional MRI (rs-fMRI) has been used to investigate T2DM-related changes in brain activity using amplitude of low-frequency fluctuation (ALFF) of the blood oxygenation level-dependent (BOLD) signal, and the changes in localized energy consumption using the regional homogeneity (ReHo) (Chen et al., 2014; Cui et al., 2014; Cui et al., 2015; Moheet, Mangia, & Seaquist, 2015; Xia et al., 2013). Other rs-fMRI studies indicated that functional interactions of certain functional systems, measured by functional connectivity (FC) based on the temporal synchronizations of BOLD signals among distinct brain regions, could also be affected (Li et al., 2020). However, these studies mainly focused on the default mode network (DMN), a large-scale resting-state functional network mediating cognitive and emotional processes (Cui et al., 2014), and did not involve other functional systems, such as the attention (Xia et al., 2015), frontoparietal, and sensorimotor networks (SMNs) (Chen et al., 2015), in which the alterations were reported in the studies afterward.

While these pioneering neuroimaging studies have provided interesting results, little is known whether the T2DM-CI, a systemic disease, could elicit functional abnormality as a widespread disease-related "pattern" encompassing the entire brain. The existing studies either focused on the voxel-by-voxel statistical comparisons (Chen et al., 2014; Cui et al., 2014; Cui et al., 2015) or limited the scope in certain predefined brain regions/subnetworks, despite the structural studies suggesting unspecific and widespread alterations (Moran et al., 2013; Schmidt et al., 2004). While network neuroscience studies with complex network analysis indicated that T2DM patients had reduced efficiency in the whole-brain structural connectivity network (Zhang et al., 2014) and the gray matter co-variation network (Cao et al., 2019) compared to healthy controls (HCs), none of them reported if such a pattern also looks alike in the whole-brain functional networks in T2DM and whether the affected connections are associated with T2DM-induced cognitive impairment. In this study, we assumed that, due to the widespread and systemic effect caused by T2DM, T2DM-CI could cause widely distributed brain functional dis-concordance. To detect such functional mis-coordination with better sensitivity, we used a recently established, dynamic (time-varying)

FC-based large-scale high-order brain network construction method [dynamics-based HOFC (dHOFC), measuring the temporal synchronization of the dynamic FC (dFC) time series among multiple region pairs] to capture the alterations in higher-level functional organization in T2DM-CI (Chen et al., 2017; Chen, Zhang, Lee, & Shen, 2017; Chen, Zhang, & Shen, 2016b; Liu et al., 2019; Zhang, Chen, Zhang, & Shen, 2017; Zhou et al., 2020). Compared to the traditional static FC (we called it "low-order" FC, or LOFC for short, to better distinguish it from the dHOFC), dHOFC has shown improved disease detection sensitivity in many studies, including mild cognitive impairment (MCI) detection. Meanwhile, instead of using the conventional link-wise statistical comparisons that may not be optimal for such a pattern detection, we used a machine learning–based multivariate pattern recognition method, to classify individual T2DM-CI from HC, so that the contributing features in the classification model could constitute a T2DM-CI abnormality "pattern" for better understanding of the diabetic encephalopathy.

In addition, previous studies did not specifically investigate T2DM-CI or try to reveal the potential differences between T2DM-CI and T2DM without cognitive impairment (T2DM-noCI). To better understand why some T2DM patients developed cognitive impairment but others not, and whether there could be "pattern differences" between T2DM-CI and T2DM-noCI, we further divided the T2DM groups into T2DM-CI group and T2DM-noCI group, with 23 and 27 patients, respectively. We separately classified them from the matched HC based on the support vector machines (SVM) using dHOFC networks as features. We hypothesized that the T2DM-CI had widespread impaired brain networks and thus could be well separated from the HC. On the contrary, we anticipated that the T2DM-noCI might not be separated from the HC as successfully as T2DM-CI did due to largely intact cognitive functions and less affected brain networks. We also hypothesized that the contributive patterns derived from the T2DM-CI versus HC were different from those derived from the T2DM-noCI versus HC classification.

2 | METHODS

2.1 | Participants

Totally, 100 participants (23 T2DM-CI, 27 T2DM-noCI, and 50 HC) were enrolled in this study from October 2018 to December 2020. This study was approved by the Ethics Committee of the First Affiliated Hospital of Guangzhou University of Chinese Medicine, Guangzhou, China. All participants had written informed consent. We divided the participants into two experiments. One experiment consisted of 23 T2DM-CI and 25 HC, while another experiment constituted of 27 T2DM-noCI and 25 different HC. Age, gender, and education level between the two groups in each experiment were matched. The HC used in the two experiments were volunteers enrolled at the same period. The T2DM patients were diagnosed at both in-patient and out-patient departments at the First Affiliated Hospital of Guangzhou University of Chinese Medicine. The diagnostic criterion is either fasting plasma glucose level ≥7.0 mmol/L or 2-hr oral glucose tolerance test glucose level ≥11.1 mmol/L, according to Association (2014). T2DM-CI was defined as the T2DM patients with a Montreal Cognitive Assessment (MoCA) score <26 (Nasreddine et al., 2005). Other cognitive tests [auditory verbal learning test (AVLT) (Schmidt, 1996), trail-making test (Bowie & Harvey, 2006), clock-drawing test (Samton et al., 2005), and digit span test (Gong, 1992)] were carried out but not included in this study because it is out of the scope of the current study. T2DM-noCI patients and all HC had MoCA scores ≥26. These diagnoses were clinically performed by two experienced endocrinologists at the First Affiliated Hospital of Guangzhou University of Chinese Medicine on a consensus basis. The exclusion criteria included history of serious brain diseases (e.g., tumor, significant brain trauma, stroke, meningitis, and cerebral infarction), psychiatric disorders (e.g., bipolar disorder, schizophrenia, generalized anxiety disorder, and major depressive disorder), history of alcohol or drug abuse, complications such as liver or kidney diseases, level-three hypertension, heart attack, and MRI contraindications.

2.2 | MRI acquisition and preprocessing

All data were collected using the same 3.0T GE scanner (SIGNA EXCITE; GE Medical Systems, Milwaukee, WI) with an eight-channel head coil. Conventional oblique axial scanning of the whole brain was performed on all subjects, including T1-weighted imaging (T1WI), T2-weighted imaging, and fluid-attenuated inversion recovery sequences. All participants were asked to lie supinely in the scanner with their heads fixed by foam pads to minimize head movement. During the scan, they were asked not to fall asleep, relax with eyes closed, and avoid deliberate thinking. We monitored the image quality and subjects during the scan and terminated the data acquisition if the images were abnormal. Sagittal high-resolution whole-brain T1WI was obtained using three-dimensional fast spoiled gradient-echo sequences [repetition time (TR) = 8.15 ms, echo time (TE) = 3.17 ms, flip angle = 12°, slice thickness = 1 mm, slice gap = 0 mm, number of excitations (NEX) = 1, field of view (FOV) = 256 mm × 256 mm, matrix size = 256 × 256), 188 sagittal slices, and 250-s total scanning time]. Blood oxygen level-dependent (BOLD) rs-fMRI data were acquired using an echo-planar imaging sequence with the following parameters: TR = 2000 ms, TE = 30 ms, flip angle = 90°, slice thickness = 3 mm, slice gap = 1 mm, FOV = 220 mm × 220 mm, matrix size = 64 × 64, 36 axial slices, and 370-s scanning time. Data Processing Assistant for rs-fMRI version 4.4 (http://rfmri.org/DPARSF) and Statistical Parametric Mapping (SPM12, http://www.fil.ion.ucl.ac.uk/spm) on MATLAB version R2016b were used to preprocess the rs-fMRI data. The preprocessing procedures were as follows: (a) discarding the first five volumes; (b) slice timing correction; (c) head motion correction; (d) spatial normalization based on unified segmentation on the co-registered T1WI and then applying the deformation field to the rs-fMRI data, before resampling the latter to 3-mm isotropic voxels (of note, more sophisticated brain registration methods

could be used in the future to improve registration accuracy across subjects (Ip & Shen, 1998; Jia, Wu, Wang, & Shen, 2010; Jia, Yap, & Shen, 2012; Patton et al., 2005; Wu, Jia, Wang, & Shen, 2011); (e) spatial smoothing with an isotropic Gaussian kernel with a full width half maximum of 6 mm in each direction; (f) removing linear trends of the rs-fMRI time series and temporal filtering with a frequency band of 0.01–0.1 Hz; and (g) regressing out Friston 24-parameter head motion parameters (Friston, Williams, Howard, Frackowiak, & Turner, 1996), mean signals from the white matter, cerebrospinal fluid, and the whole brain (i.e., global signal). All subjects had head motion <2 mm (translation in any direction) and 2° (rotation in any direction), and mean framewise displacement (FD) <0.5 mm (Power et al., 2014; Power, Barnes, Snyder, Schlaggar, & Petersen, 2012).

2.3 | Classification based on high-order FC networks

We used Brain Network Construction and Network-based Classification toolbox (BrainNetClass v1.1, Zhou et al., 2020) to construct brain dHOFC networks for all subjects (23 T2DM-CI from 25 HC) and classify the subjects in the two groups. Similar analysis and classification were conducted for 27 T2DM-noCI and 25 HC (see Figure 1). BrainNetClass is a Matlab-based, automatic, easy-to-use pipeline for advanced brain network construction and network-based disease classification (https://github.com/zzstefan/BrainNetClass). We chose "dHOFC" as the brain network construction method because the previous studies indicated that such a method could better capture disease-related subtle changes and outperform traditional (low-order) FC in disease classification (Chen, Zhang, & Shen, 2016b; Liu et al., 2019; Zhang et al., 2017; Zheng et al., 2019). The procedure was well documented elsewhere (Chen, Zhang, & Shen, 2016b; Zhou et al., 2020) and only briefly described below. After regional averaged rs-fMRI time series were extracted from each of the 116 regions-of-interest (see their abbreviations and full names in Supplementary Table 1) according to the automated anatomical labeling (AAL) atlas, we calculated dFC between each pair of regions using a well-adopted sliding window correlation approach, with a step size of one TR and a window length optimized as below (Preti, Bolton, & Van De Ville, 2017). The dFC time series were concatenated across all subjects and the hierarchical clustering was used to group synchronized dFC time series into clusters. The resultant cluster centroids (i.e., the representative dFC time series of each cluster) were then fed into a second round of Pearson's correlation analysis to generate a dHOFC matrix for each subject. Therefore, each new "node" in the dHOFC network represents a set of pairwise inter-regional links with highly

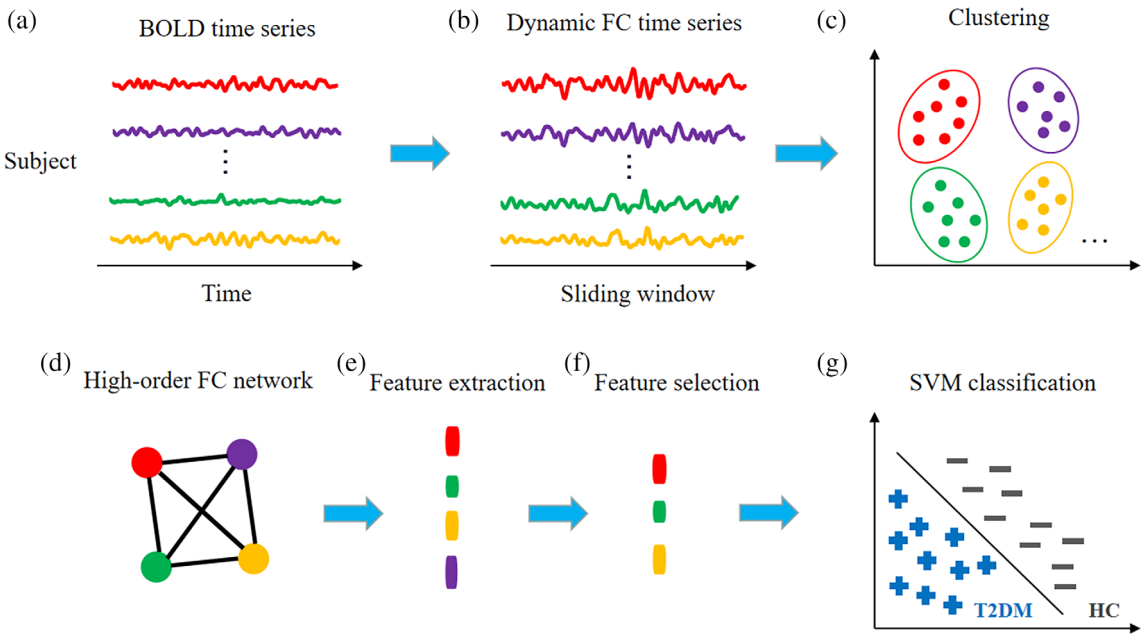

FIGURE 1 Framework of dynamics-based high-order functional connectivity (dHOFC) network construction and network-based classification between type 2 diabetes mellitus with cognitive impairment (T2DM-CI) and the healthy controls (HC). The framework for classification between type 2 diabetes mellitus without cognitive impairment (T2DM-noCI) and the HC is the same. The training phase starts with sliding window-based dynamics functional connectivity (dFC) analysis (b) for all the region pairs based on the BOLD time series extracted from the automated anatomical labeling (AAL) template (a). After concatenating all subjects' dFC time series, k-means clustering is conducted to group the dFC time series into clusters (c), before a second round of Pearson's correlation analysis between any pair of cluster-averaged dFC time series for constructing dHOFC network (d). Nodal clustering coefficients are extracted from all the nodes in the dHOFC network construction as features (e). After a feature selection based on Least Absolute Shrinkage and Selection Operator (LASSO) (f), a support vector machine (SVM) model is built for classification (g). In the testing phase (not shown in the figure), the testing sample that was left out is used and the same features are selected before they are fed into the trained classification model for generating the predicted label

synchronized dFC profiles. Each new "link" in the dHOFC network represents the coordination between each pair of these new "nodes" in the dHOFC network, which may reflect a high-order brain functional organization. Of note, this high-order FC differs from the conventional low-order FC (LOFC) based on the traditional Pearson's correlation on raw BOLD rs-fMRI signals.

For each node in the dHOFC network, we calculated its local clustering coefficient as features based on the weighted networks (Chen, Zhang, & Shen, 2016), as previously done for LOFC networks (Bassett & Bullmore, 2006). This complex network metric quantified the probability that a node's neighbors in the dHOFC network also connected with each other, reflecting nodal local efficiency of the dHOFC network (Bassett & Bullmore, 2006). Due to possible feature redundancy, we adopted the Least Absolute Shrinkage and Selection Operator (LASSO) to select only crucial features to improve the classification performance and model robustness (Tibshirani, 1996). Altogether, there were three freely estimable parameters to be optimized, including the window length for sliding window correlation, the number of clusters for deciding the effective number of nodes in the dHOFC, and the LASSO parameter that controlled the number of selected features. They were optimized from the ranges of [20, 30, …, 60], [100, 200, …, 800], and [0.07, 0.075, …, 0.09], respectively, by using a nested leave-one-out cross-validation (LOOCV) strategy.

During the nested LOOCV, an inner LOOCV was used for parameter optimization and an outer LOOCV was for model evaluation with the optimized parameters. We trained a SVM to perform classification. SVM is a well-validated and extensively used classifier with superior performance even with a small sample size (Zeng et al., 2012; Zhou et al., 2020; Zhou, Wang, Zang, & Pan, 2018), which is suitable for our experiments. SVM searches for optimal hyperplane that separates the critical elements (i.e., support vectors) mapped to a high-dimensional space with certain kernels (Cortes & Vapnik, 1995; Misaki, Kim, Bandettini, & Kriegeskorte, 2010). In this article, we used a linear kernel and the hyperparameter C was set to 1. After the LOOCV procedure was repeated and all subjects were gone through it, various performance evaluation metrics were derived comparing the predicted label with the ground truth. These metrics include the area under the curve (AUC) of receiver operator characteristics, accuracy, sensitivity, specificity, and F1-score (Sokolova, Japkowicz, & Szpakowicz, 2006). To compare the results with that from the LOFC, we also built traditional Pearson's correlation-based network (termed as LOFC) and conducted LOFC-based classification using BrainNetClass toolbox (by selecting Pearson's correlation as the network construction method in the toolbox). We used the connection coefficients of the constructed LOFC network as features and applied two-sample *t*-test with LASSO for feature selection (Zhang et al., 2019). The SVM classifiers with the same settings were used to perform the classification with LOOCV.

2.4 | Identification of discriminative features

To find and compare potential contributing features of the classification between T2DM-CI and HC, and the classification between T2DM-noCI and HC, we identified discriminative dHOFC nodes (i.e., a set of pairwise inter-regional links with highly synchronized dFC profiles) according to their frequency of being selected during the outer LOOCV runs. The more frequently the feature was selected, the more important this feature could be (Liu et al., 2019). Then, we selected and illustrated the most discriminative features (those with the selection frequency >95%). To further evaluate which large-scale functional network(s) these coordinated dFC links encompassed, for each discriminative dHOFC node, we checked each brain region's network affiliation, according to the network templates in Yeo et al. (2011) for cerebral regions and Buckner, Krienen, Castellanos, Diaz, and Yeo (2011) for cerebellar regions. Specifically, each AAL region was assigned to one of the seven large-scale brain functional networks: frontoparietal network (FPN), ventral attention network (VAN), DMN, dorsal attention network (DAN), SMN, visual network (VN), and limbic/basal ganglia network (LN) (Tzourio-Mazoyer et al., 2002).

2.5 | Statistical analysis

Statistical analysis of the clinical and neuropsychological data was performed using Stata 11.0 (Stata, College Station, TX). Between-group comparisons were conducted between T2DM-CI and HC as well as between T2DM-noCI and HC by using two-sample *t*-tests or Mann–Whitney nonparametric tests depending on whether the variables satisfied normal distribution and variance homogeneity. Gender differences were examined by chi-square tests. To investigate the associations between imaging features (i.e., local clustering coefficients of the discriminative dHOFC nodes) and clinical symptoms [i.e., MoCA scores and AVLT (immediate recall) (AVLT-IR)], we performed multiple linear regression by using SPSS v23.0 (Chicago, IL) after controlling other confounding demographic variables (i.e., age, gender, and education level). Specifically, each imaging feature was included as an independent variable, while MoCA score and AVLT-IR were included as a dependent variable, and age, gender, and education level as covariates. We also calculated partial correlation between each imaging feature and MoCA score, as well as AVLT-IR. The results with $p < .05$ were considered as statistically significant.

3 | RESULTS

3.1 | Information and comparison of clinical and neuropsychological data

The information of the clinical and neuropsychological data of the 100 participants was summarized in Table 1, where the characteristics showing significant group differences ($p < .05$) were marked with asterisk. Statistical comparisons between the T2DM-CI and HC (and between T2DM-noCI and HC) revealed no significant differences in age, gender, or education level. Some clinical characteristics such as blood pressure showed significant differences both between T2DM-CI and HC and between T2DM-noCI and HC. MoCA scores and AVLT-IR showed significant differences between the T2DM-CI

TABLE 1 Comparison of clinical and neuropsychological characteristics between two groups

	T2DM-CI ($n = 23$)	HC ($n = 25$)	p value	T2DM-noCI ($n = 27$)	HC ($n = 25$)	p value
Clinical characteristics						
Age (years)	54.87 ± 9.13	54.24 ± 4.83	.43	47.81 ± 8.75	50.72 ± 6.15	.18
Gender (M/F)	8/15	12/13	.39	21/6	17/8	.54
Education (years)	8.00 ± 4.67	8.96 ± 3.74	.43	11.78 ± 3.18	12.48 ± 2.80	.40
Fasting plasma glucose (mmol/L)	8.81 (7.19–10.30)	4.88 (4.50–5.30)	.0001*	7.55 ± 1.93	4.66 ± 0.57	.0001*
BMI (kg/m^2)	24.52 ± 2.57	23.20 ± 2.56	.082	24.47 ± 2.78	22.89 ± 2.50	.037*
HbA1c (%)	9.37 ± 1.77	NA	NA	8.92 ± 2.33	NA	NA
Systolic blood pressure (mm Hg)	128.26 ± 13.88	116.64 ± 9.29	.0013*	125.63 ± 12.91	116.40 ± 9.48	.0053*
Diastolic blood pressure (mm Hg)	80.48 ± 8.61	75.64 ± 5.78	.026*	83.59 ± 9.89	76.72 ± 5.40	.013*
TC (mmol/L)	4.65 ± 1.02	NA	NA	4.62 ± 0.97	NA	NA
TG (mmol/L)	2.05 (1.25–2.37)	NA	NA	1.90 (0.96–3.10)	NA	NA
LDL (mmol/L)	3.41 ± 1.13	NA	NA	3.03 ± 0.95	NA	NA
Neuropsychological characteristics						
MoCA	21.74 (18–25)	27.08 (26–28)	.0001*	27.63 ± 1.28	27.92 ± 1.38	.43
AVLT-IR	16.87 ± 4.55	20.68 ± 4.31	.0046*	22.26 (20–26)	21.20 (18–26)	.36
AVLT-STR	6.65 ± 2.71	7.76 ± 1.71	.093	7.70 ± 1.64	7.88 ± 1.99	.73
AVLT-LTDR	6.74 ± 3.39	7.60 ± 1.66	.29	7.93 ± 1.57	7.48 ± 2.06	.38
TMT-A	77.17 (53–95)	64.60 (55–69)	.36	61.50 (59–69)	61.18 (56–66)	.17
TMT-B	61.56 (45–72)	59.47 (51–67)	.98	61.57 (49–65)	56.17 (45–64)	.51
DST	11.43 ± 1.78	11.80 ± 1.89	.50	11.04 ± 1.26	11.32 ± 1.31	.43
CDT	2.70 (2–3)	2.72 (2–3)	.73	2.85 (2–3)	2.92 (2–3)	.67

Abbreviations: T2DM-CI: type 2 diabetes mellitus with cognitive impairment; T2DM-noCI: type 2 diabetes mellitus without cognitive impairment; HC: healthy controls; M: male; F: female; MoCA: Montreal cognitive assessment; BMI: body mass index; TC: total cholesterol; TG: triglycerides; LDL: low-density lipoprotein; AVLT: auditory verbal learning test; AVLT-IR: auditory verbal learning test (immediate recall); AVLT-STR: auditory verbal learning test (short-term recall after 5 min); AVLT-LTDR: auditory verbal learning test (long-term delayed recall after 20 min); TMT: trail-making test; DST: digit span test; CDT: clock-drawing test.

TABLE 2 Classification performance in T2DM-CI versus HC and T2DM-noCI versus HC differentiation

Group	Method	AUC	ACC (%)	SEN (%)	SPE (%)	F1-score (%)
T2DM-CI vs. HC	dHOFC	0.81	79.17	69.57	88.00	76.19
	LOFC	0.63	56.25	39.13	72.00	46.15
T2DM-noCI vs. HC	dHOFC	0.68	59.62	55.56	64.00	58.82
	LOFC	0.58	51.92	48.00	55.56	48.98

Abbreviations: T2DM-CI: type 2 diabetes mellitus with cognitive impairment; T2DM-noCI: type 2 diabetes mellitus without cognitive impairment; HC: healthy controls; AUC: area under curve; ACC: accuracy; SEN: sensitivity; SPE: specificity; dHOFC: dynamics-based high-order functional connectivity; LOFC: low-order functional connectivity.

patients and their matched HC but not between the T2DM-noCI patients and their matched HC. For other neuropsychological characteristics, they showed no significant differences between the T2DM-noCI patients and the matched HC.

3.2 | Classification performance

The performance comparison between the classification models using dHOFC and LOFC was shown in Table 2. The dHOFC-based classification performance in both T2DM-CI versus HC and T2DM-noCI versus HC classification was better than that of LOFC with respect to all the performance metrics. Generally, the use of dHOFC boosted T2DM-CI versus HC classification accuracy by ~23% (79.17%), with balanced sensitivity (69.57%) and specificity (88.00%), compared to that using LOFC. In contrast, dHOFC-based classification between T2DM-noCI and HC led to less accurate (59.62% in accuracy) results. Again, its performance was still higher than that of the LOFC-based classification (51.92% in accuracy).

3.3 | Top discriminative dHOFC features in T2DM-CI versus HC classification

We identified two dHOFC nodes with their local clustering coefficients as discriminative features in the classification of T2DM-CI from HC. To generate interpretable spatial configurations of the dHOFC nodes and visualize them, we showed the brain region pairs with covaried dFC from the two dHOFC nodes in Figure 2 (see the details of the pairwise connections involved in Supplementary Table 2). These regions and connections involved time-varying coordination across all the large-scale brain networks (see the LN involved in Supplementary Figure 1).

Specifically, the node 1 (selected in a frequency of 95.83% from all the LOOCV runs) in dHOFC encompassed the SMN, DMN, and VAN. It contained 50 links, 22 out of which were the intra-network connections in the SMN. The involved connections were among the left median cingulate and paracingulate gyri (DCG.L), right median cingulate and paracingulate gyri (DCG.R), left Rolandic operculum (ROL.L), right Rolandic operculum (ROL.R), left supramarginal gyrus (SMG.L), right supramarginal gyrus (SMG.R), left superior temporal gyrus (STG.L), right superior temporal gyrus (STG.R), right supplementary motor area (SMA.R), left insula (INS.L), right insula (INS.R), right precentral gyrus (PreCG.R), left postcentral gyrus (PoCG.L), right postcentral gyrus (PoCG.R), left Heschl's gyrus (HES.L), and right Heschl's gyrus (HES.R). As for the brain region's affiliation to each large-scale brain functional network, we calculated the ratio between the number of regions belonging to each functional network and the total number of the regions in that functional network, which was used to indicate the functional system's relative involvement of the discriminative node in dHOFC (as shown in the right panel in Figure 2). We also calculated the absolute involvement of each functional network by counting the summed "degree" of all the regions in each functional network from the "cluster" of links [(a node in the dHOFC network) shown in the left panel in Figure 2]. In the node 1, the SMN accounted for 75% relative involvement with an absolute involvement degree of 68, while the involvement of the other two high-level systems (DMN and VAN) was relatively small (12.5% relative involvement and their sum of absolute involvement degree was 16, respectively).

The node 2 (selected in the same frequency as that of the node 1) in dHOFC encompassed more functional systems than the node 1, including both primary (SMN and VN) and high-level (DMN, FPN, DAN, and VAN) systems. Among 48 links, 46 were inter-network connections. The connections involved the left paracentral lobule (PCL.L), right paracentral lobule (PCL.R), left calcarine fissure and surrounding

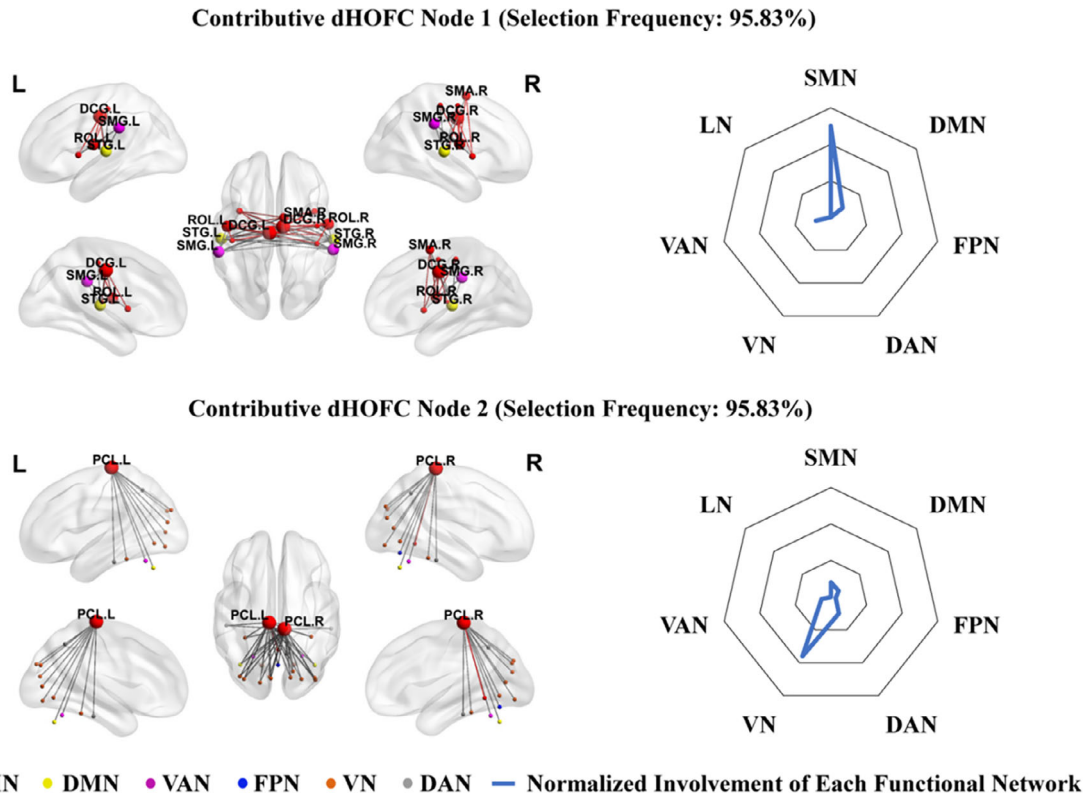

FIGURE 2 The left panel shows the top two discriminative dynamics-based high-order functional connectivity (dHOFC) nodes selected from classification between type 2 diabetes mellitus with cognitive impairment (T2DM-CI) and healthy controls (HC) according to the selection frequency (95.83%). The colored nodes represent brain regions in different large-scale brain networks derived from Yeo et al. (2011) and Buckner et al. (2011). The node size reflects the number of involved highly co-varied dFC links with other regions. The color of the links represents intra-network connections (in respective network's color) or inter-network connections (gray). The right panel shows the radar maps of the relative involvement of each dHOFC node with respect to seven large-scale functional networks

cortex (CAL.L), right calcarine fissure and surrounding cortex (CAL.R), left cuneus (CUN.L), right cuneus (CUN.R), left lingual gyrus (LING.L), right lingual gyrus (LING.R), left superior occipital gyrus (SOG.L), right superior occipital gyrus (SOG.R), left middle occipital gyrus (MOG.L), right middle occipital gyrus (MOG.R), left inferior occipital gyrus (IOG.L), right inferior occipital gyrus (IOG.R), left fusiform gyrus (FFG.L), right fusiform gyrus (FFG.R), left precuneus (PCUN.L), right precuneus (PCUN.R), left inferior temporal gyrus (ITG.L), right inferior temporal gyrus (ITG.R), left cerebellum crus1 (CRBLCrus1.L), right cerebellum crus1 (CRBLCrus1.R), left cerebellum6 (CRBL6.L), right cerebellum6 (CRBL6.R), vermis45 (Ver45), and vermis6 (Ver6). According to the relative involvement, the VN (53.85%) was mostly involved, followed by DAN (15.38%), SMN (11.54%), DMN (7.69%), VAN (7.69%), and FPN (3.85%). However, the SMN had the highest absolute involvement degree (50), followed by VN (28), DAN (8), DMN (4), VAN (4), and FPN (2). Most of the synchronized dFC links involved bilateral paracentral lobules.

For other discriminative nodes in the dHOFC network with lower (but still high, between 90% and 95%) selection frequency, please see Supplementary Figure 1. Please note that we did not show the LOFC features derived from the classification between T2DM-CI and HC because of its low accuracy.

3.4 | Association between dHOFC features and clinical variables

We found a relationship between brain dHOFC features (i.e., local clustering coefficient of the top discriminative dHOFC nodes 1 and 2) and clinical features (i.e., MoCA scores, reflecting general cognitive function) based on partial correlation analysis in the T2DM-CI group. Specifically, local clustering coefficient of the dHOFC node 1, together with three covariates (age, gender, and education level) successfully explained the MoCA scores in the T2DM-CI group, as evaluated by multiple regression ($p = .005$). With partial correlation analysis (after adjusting for the effect of the covariates), their association was significant ($r = .444$, $p = .050$, Figure 3a). We also found that MoCA scores were correlated with education level ($r = .672$, $p = .001$). For dHOFC node 2, we also found that MoCA scores can be successfully explained by the dHOFC feature and three covariates ($p = .002$). Partial correlation indicated a nearly significant relationship between the local clustering coefficient of the dHOFC node 2 and MoCA scores ($r = .437$, $p = .054$, Figure 3b). We also found that MoCA scores were correlated with education level ($r = .597$, $p = .005$).

3.5 | Top discriminative dHOFC features in T2DM-noCI versus HC classification

We also identified top one dHOFC node (selected in a frequency of 90.38% from all the LOOCV runs) with their local clustering coefficients as discriminative features in the classification of T2DM-noCI from HC (Figure 4). Compared to T2DM-CI, the regions, and connections of T2DM-noCI encompassing the SMN, and FPN, may not involve large-scale brain networks. It contained 16 links, half of which were the intra-network connections in the FPN, while others were inter-network connections. The involved connections were among the orbital part of the left superior frontal gyrus (ORBsup.L), the orbital part of the right superior frontal gyrus, (ORBsup.R), the orbital part of the left middle frontal gyrus (ORBmid.L), the orbital part of the

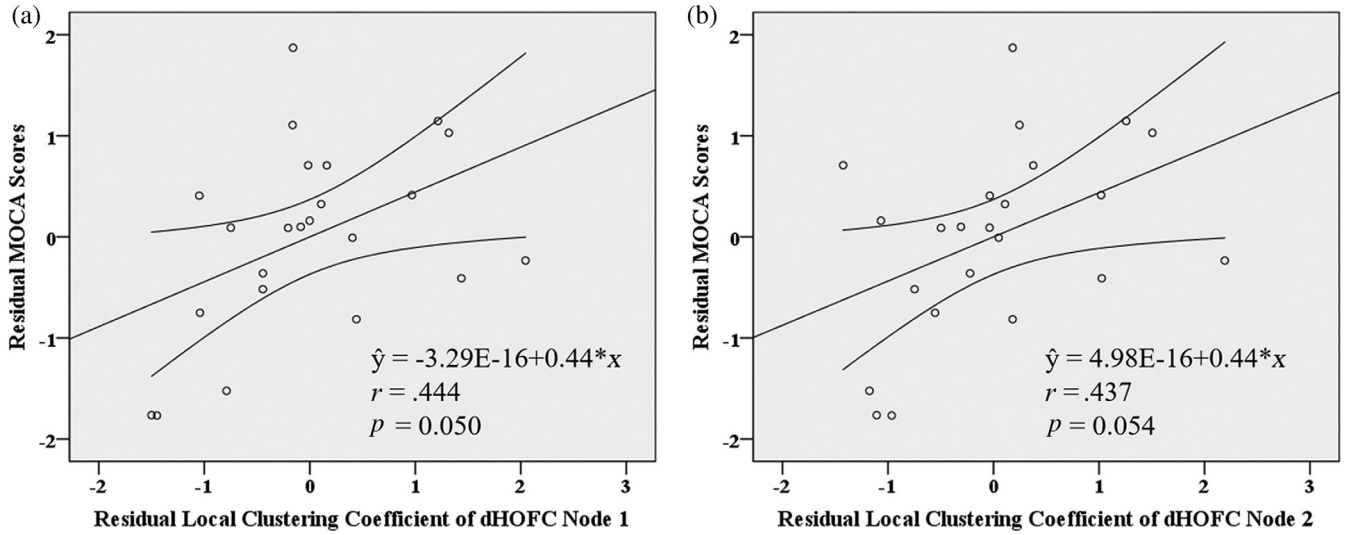

FIGURE 3 Scatter plots of the dynamics-based high-order functional connectivity (dHOFC) features [(a) and (b) represent the local clustering coefficients of the dHOFC node 1 and node 2, respectively, shown in Figure 2] against Montreal Cognitive Assessment (MoCA) scores in the group of type 2 diabetes mellitus with cognitive impairment (T2DM-CI). Both values were corrected by removing the effect of age, gender, and education level. The straight lines denoted fitted lines, and the curves on both sides were the 95% confidence interval. The *P* and *r* values were derived from partial correlation analysis

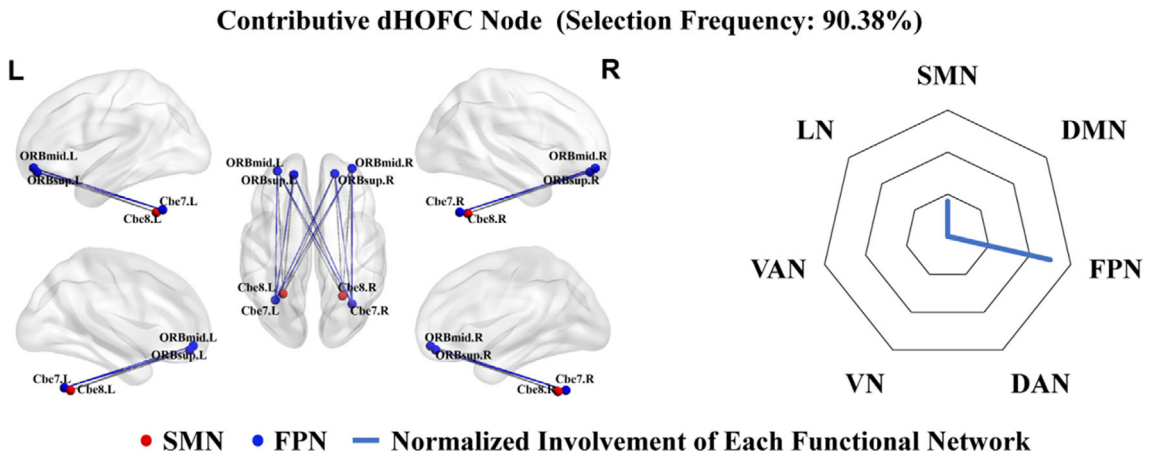

FIGURE 4 The left panel shows top one discriminative dynamics-based high-order functional connectivity (dHOFC) nodes selected from classification between type 2 diabetes mellitus without cognitive impairment (T2DM-noCI) and healthy controls (HC) according to the selection frequency (90.38%). The colored nodes represent brain regions in different large-scale brain networks derived from Yeo et al. (2011) and Buckner et al. (2011). The node size reflects the number of involved highly co-varied dFC links with other regions. The color of the links represents intra-network connections (in respective network's color) or inter-network connections (in gray). The right panel shows the radar maps of the relative involvement of each dHOFC node with respect to seven large-scale functional networks

right middle frontal gyrus (ORBmid.R), left cerebellum region 7b (CRBL7b.L), right cerebellum region 7b (CRBL7b.R), left cerebellum region 8 (CRBL8.L), and right cerebellum region 8 (CRBL8.R) (see the details of the pairwise connections involved in Supplementary Table 3). According to the relative involvement and absolute involvement degrees, the FPN (75%, 24) was mostly involved, while SMN was relatively small (25%, 8).

3.6 | Association between dHOFC features and clinical variables

We found a relationship between brain dHOFC features (i.e., local clustering coefficient of the top discriminative dHOFC node) and clinical features (i.e., AVLT-IR, reflecting short-term memory) based on partial correlation analysis in the T2DM-noCI group. Specifically, local clustering coefficient of the dHOFC node, together with three covariates (age, gender, and education level), successfully explained the AVLT-IR in the T2DM-noCI group, as evaluated by multiple regression ($p = .000$). With partial correlation analysis (after adjusting for the effect of the covariates), their association was significant ($r = -.459$, $p = .024$, Figure 5). We also found that AVLT-IR was correlated with education level ($r = .430$, $p = .036$).

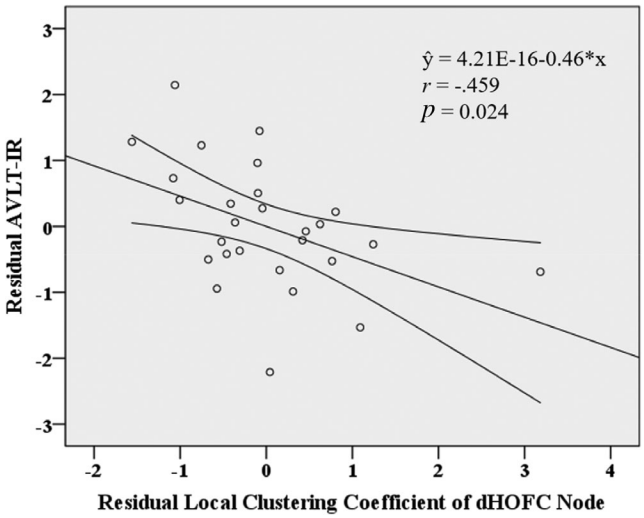

FIGURE 5 Scatter plots of the dynamics-based high-order functional connectivity (dHOFC) node feature against the auditory verbal learning test (immediate recall) (AVLT-IR) in the group of type 2 diabetes mellitus without cognitive impairment (T2DM-noCI). The values were corrected by removing the effect of age, gender, and education level. The straight lines denoted fitted lines, and the curves on both sides represented the 95% confidence interval. The *P* and *r* values were derived from partial correlation analysis

4 | DISCUSSIONS

To the best of our knowledge, this is the first classification study between T2DM-CI and HC as well as T2DM-noCI and HC based on brain functional network. We used brain dHOFC network to increase the sensitivity in detection of disease-induced brain functional changes. The results indicate that there exists discriminative synchronization of dFC across large-scale intrinsic brain networks that can differentiate T2DM-CI (and T2DM-noCI) from HC. By building dHOFC network and conducting network-based classification with the help of machine learning, we, for the first time, revealed a few covaried dFC that were associated with T2DM-induced cognitive impairment, some of which significantly correlated with patients' cognitive abilities as assessed by MoCA and AVLT-IR. The dHOFC-based classification between

T2DM-noCI and HC was not as good as that between T2DM-CI and HC, together with different dHOFC features, which indicated that T2DM-CI involved severe brain functional disorders that could be different from T2DM-noCI. Our findings provide valuable information that may help to understand T2DM-related alterations in the central neural system.

Our study indicates that dHOFC can be a good metric to model the complex interactions among brain regions and capture high-level cognitive functions, compared to the traditional, LOFC (79.17% vs. 56.25% in accuracy). It further confirms that dHOFC can be very sensitive to MCI, as found in previous MCI detection studies (Chen, Zhang, & Shen, 2016b). Of note, similar finding is found in the classification between T2DM-noCI and HC. Despite some studies (El-Baz, Hassanien, & Schaefer, 2016; Yue, Xin, Kewen, & Chang, 2008) have used machine learning to diagnose diabetes based on simple clinical features, such as personal data and results of medical examinations, our study highlights the value of brain functional imaging in T2DM diagnosis, especially in evaluation of cognitive decline caused by T2DM. Compared with other functional imaging metrics, such as ReHo and ALFF also derived from rs-fMRI, dHOFC measures long-range functional interactions in a time-varying manner and captures their synchronizations, and thus can be more sensitive to subtle changes in the cognitive status.

To perform a preliminary (due to unmatched age, gender, and education level) comparison between the two T2DM groups for a better understanding of T2DM-related cognitive impairment, we performed one more classification task between 23 T2DM-CI and 27 T2DM-noCI using dHOFC. This classification achieved an ACC of 66.00%, while the AUC, SEN, SPE, and F1-score were 0.66, 56.52%, 74.07%, and 60.47%, respectively. This result shows a degraded but still to-some-extent possible separation between T2DM-CI and T2DM-noCI groups. Since the T2DM-CI and T2DM-noCI groups had the same underlying disease (i.e., T2DM), we considered that T2DM per se could cause more significant changes in the brain functional networks than T2DM-related CI does. This might lead to less accurate classification results between T2DM-CI and T2DM-noCI. Furthermore, we hypothesized that T2DM-CI had widespread brain network impairment while T2DM-noCI also had similar (but possibly less) affected brain networks; therefore, we could not separate them as well as separating T2DM-CI from HC. We detected three shared networks (i.e., SMN, DMN, and VAN) that could be more affected in T2DM-CI compared with T2DM-noCI, while the possible affected brain networks as revealed by T2DM-noCI versus HC classification did not include VN, DAN, DMN, and VAN. Please be also noted that SMN and VN were found to have an important role in the classification between T2DM-CI and HC, while FPN ranked the top in the classification between T2DM-noCI and HC. This new experiment suggests that the DMN could be vital in the classification between T2DM-CI and T2DM-noCI. Meanwhile, we also found that the SMN is the network that might be involved in all three classifications. Therefore, we think that further impaired DMN could be related to T2DM-related CI.

Our study, in consistent with previous rs-fMRI studies, suggests that the functional alteration in the DMN may play a role in cognitive decline in patients with T2DM. Previous studies showed that T2DM-related impaired FC was mainly in the DMN (Cui et al., 2015; Musen et al., 2012; Xia et al., 2015; Yang et al., 2016; Zhou et al., 2010). Yang et al. (2016) also found reduced FC in patients with T2DM-induced MCI between the DMN and other regions, while a few other studies reported reduced FC between the DMN regions and anterior cingulate cortex (Zhang et al., 2015), FFG.L (Musen et al., 2012), right inferior frontal gyrus (IFG.R), and left thalamus (Zhou et al., 2010). In resting state, the DMN is one of the most active brain systems that is closely related to internal recognition (i.e., episodic memory, theory of mind, and self-evaluation) (Buckner, Andrews-Hanna, & Schacter, 2008; Sestieri, Corbetta, Romani, & Shulman, 2011). It is very important that a dynamic balance of the interactions among regions inside the DMN as well as those between the DMN and other brain systems to maintain a normal cognitive function (Uddin, Clare Kelly, Biswal, Xavier Castellanos, & Milham, 2009). Patients with T2DM are generally at a higher risk of cognitive impairment; therefore, they may show altered dHOFC in the DMN.

Another important finding in our article is the strong involvement of the SMN in T2DM-CI. Of note, we also find that the SMN is informative in the T2DM-noCI diagnosis. Motor area, such as the precentral gyrus, is associated with motor (Mattingley, Husain, Rorden, Kennard, & Driver, 1998) and cognitive decline in previous MRI studies of diabetic patients (Cui et al., 2014; Manschot et al., 2006; Wang, Fu, Liu, Xing, & Zhang, 2014). SMN is generally believed to be responsible for motor and somatosensory functions (Barber et al., 2012). However, it is also considered to be involved in some high-order cognitive functions, such as episodic memory, action recognition, spatial navigation (Russ, Mack, Grama, Lanfermann, & Knopf, 2003), planning and execution of voluntary movements (Ferri, Frassinetti, Ardizzi, Costantini, & Gallese, 2012), and motor-learning (Singh et al., 2015). Due to the close interaction between the SMN and other functional systems, we think that the SMN can be a signature of T2DM-CI when dFC, instead of static FC, is used in the study.

We find that the VN (especially in the dHOFC node 2) can be affected in T2DM-CI patients. This is consistent with previous findings from T2DM patients using other functional metrics, such as ReHo and ALFF. For example, reduced performance in cognitive tests was found to be associated with reduced ReHo and ALFF in the cuneus and lingual gyri in T2DM patients, which could be related to impaired visual memory and word processing function (Mechelli, Humphreys, Mayall, Olson, & Price, 2000). Reduced ReHo was also found in the bilateral lingual gyrus, postcentral gyrus, parietal regions, right fusiform gyrus, precentral gyrus, and superior frontal gyrus in T2DM patients (Cui et al., 2014; Liu et al., 2016; Peng et al., 2016). Previous fMRI studies indicated that decreased brain activity in the occipital area and postcentral gyrus was related to visual impairment (Liu et al., 2011) and sensory loss (Luo et al., 2012), respectively. Diabetic retinopathy has been linked to accelerated cognitive decline and abnormal neural function (Hugenschmidt et al., 2014; Wang et al., 2017). Since the homology between retinal and cerebrovascular cells, the state of small vessels in the retina closely mirrors that of the cerebral microvasculature, suggesting that diabetic retinopathy can be used as a marker for the presence of microangiopathy within the brain

(Feinkohl, Price, Strachan, & Frier, 2015). Previous studies demonstrated many shared morphological and physiological properties between the retinal and cerebral microvasculature (Patton et al., 2005), suggesting that the microvascular changes might be related to retinopathy and changes in cognitive function. Diabetic retinopathy may be a putative marker for cognitive impairment in patients with diabetes, where the cerebral microvascular disease may have an important pathogenic role. In our study, most of the patients do not have clinical visual or sensory changes, suggesting that abnormal neural activity may be an early sign before the appearance of clinically measurable symptoms. In future work, we will further collect sensorimotor and visual disability information on testing. It will be interesting to follow these patients over time to determine the clinical significance of these findings.

We think that the interaction of multiple high-level functional networks can be altered by T2DM. A growing body of researches have demonstrated that functional disconnections among the high-level networks are responsible for cognitive impairment (Chen et al., 2015; Dai et al., 2015; Shu et al., 2012; Wang et al., 2013; Whitwell et al., 2011). In our study, we also detect altered dHOFC in such high-level resting-state networks (i.e., DMN, VAN, FPN, and DAN). DAN maybe related to some higher-level cognitive processes, such as visuospatial and executive functions (Corbetta, Kincade, & Shulman, 2002). In addition to our findings in the T2DM-CI patients, DMN, DAN, and VAN have also been found deteriorated in other cognitive impairment disorders, such as AD and hepatic encephalopathy (Fox, Corbetta, Snyder, Vincent, & Raichle, 2006; Wilson et al., 2017). It is known that the FPN is vital to working memory and other executive functions (Nielsen et al., 2017). It has been proved that the FPN has a higher degree of FC compared to other brain networks, indicating its functional diversity and roles in information integration (Marek, Hwang, Foran, Hallquist, & Luna, 2015; Power, Schlaggar, Lessov-Schlaggar, & Petersen, 2013).

Although T2DM and AD appear to share progressive cognitive impairment, the brain damage could be different. First, compared with previous early AD studies (Chen, Zhang, Gao, et al., 2016) that showed dHOFC alterations in the lateral and medial temporal gyrus, orbitofrontal cortex, superior and inferior parietal lobules, our results based on T2DM-CI revealed quite different altered regions, such as the SMN and VN that were highly ranked in the discriminative dHOFC nodes 1 and 2. Of note, we also found that the SMNs were informative in the diagnosis of T2DM-noCI. Therefore, it is not likely that our findings were related to AD. However, we did find that the education level was positively correlated with MoCA scores and AVLT-IR, which might indicate that T2DM with higher education could have better preserved cognitive ability. Longitudinal studies are needed to study whether high education could slow the progression of cognitive impairment in T2DM.

There are several limitations to our study. First, the sample size in our study was relatively small. A larger sample size is urgently needed to validate our findings. Multicenter and collaborative large databases are encouraged in the future for result validation. Second, we found that the T2DM-noCI group was more highly educated and had a lower HbA1c level that might indicate better diabetic control than the T2DM-CI group. The possible separation (ACC = 66%) between the two groups might be related to such factors. It is also difficult to evaluate whether the missing contribution of the DMN in the T2DM-noCI versus HC classification was caused by higher education in the T2DM-noCI group. Lower education level might be a vulnerability factor in normative aging and an independent risk factor of MCI or dementia. Our result shows that it could be also a possible associated factor in T2DM-related CI. Meanwhile, better diabetic control could be another reason for less-affected cognitive abilities in the T2DM-noCI. In the future, we will conduct a study with better control of the two confounding factors and classify between well-matched T2DM-CI and T2DM-noCI patients. We will also investigate the influence of education level on both groups. Third, due to the unmatched age, gender, and education level between T2DM-CI and T2DM-noCI, it is difficult to compare the differences directly between these two groups. Although we achieved an accuracy of 66% when separating T2DM-CI from T2DM-noCI, a one-on-one match in the collection of T2DM-CI- and T2DM-noCI participants should be the direction of our future efforts to better reduce the effect of age, gender, and education level. Fourth, different treatment strategies might have exerted certain effect on the results and were not considered in our study. Therefore, how to eliminate the influence of medicine should be further investigated.

5 | CONCLUSIONS

This is the first classification study between T2DM with different cognitive levels and HCs. With powerful machine learning and advanced brain functional network strategies, we managed to identify brain functional abnormalities in various brain networks, especially the sensorimotor and VNs. We found that the dynamics-based high-order FC could achieve satisfactory classification accuracy for T2DM-CI. Our findings provide valuable knowledge for better understanding of diabetes-related cognitive impairment.

CONFLICT OF INTEREST

The authors declare no potential conflict of interest.

DATA AVAILABILITY STATEMENT

I confirm that my article contains a Data Availability Statement even if no data is available (list of sample statements) unless my article type does not require one.

ORCID

Yuna Chen https://orcid.org/0000-0002-1609-4238
Jing Xia https://orcid.org/0000-0003-4962-2604

REFERENCES

American Diabetes Association. (2014). Diagnosis and classification of diabetes mellitus. *Diabetes Care*, *37*(Supplement 1), S81–S90.

Atlas, D. (2015). *International diabetes federation. IDF diabetes atlas*. Brussels: International Diabetes Federation.

Barber, A. D., Srinivasan, P., Joel, S. E., Caffo, B. S., Pekar, J. J., & Mostofsky, S. H. (2012). Motor "dexterity"?: Evidence that left

hemisphere lateralization of motor circuit connectivity is associated with better motor performance in children. *Cerebral Cortex*, *22*(1), 51–59.

Bassett, D. S., & Bullmore, E. (2006). Small-world brain networks. *The Neuroscientist*, *12*(6), 512–523.

Biessels, G. J., Staekenborg, S., Brunner, E., Brayne, C., & Scheltens, P. (2006). Risk of dementia in diabetes mellitus: A systematic review. *The Lancet Neurology*, *5*(1), 64–74.

Biessels, G. J., Strachan, M. W., Visseren, F. L., Kappelle, L. J., & Whitmer, R. A. (2014). Dementia and cognitive decline in type 2 diabetes and prediabetic stages: Towards targeted interventions. *The Lancet Diabetes & Endocrinology*, *2*(3), 246–255.

Bowie, C. R., & Harvey, P. D. (2006). Administration and interpretation of the trail making test. *Nature Protocols*, *1*(5), 2277–2281.

Brundel, M., van den Heuvel, M., de Bresser, J., Kappelle, L. J., Biessels, G. J., & Utrecht Diabetic Encephalopathy Study Group. (2010). Cerebral cortical thickness in patients with type 2 diabetes. *Journal of the Neurological Sciences*, *299*(1–2), 126–130.

Buckner, R. L., Andrews-Hanna, J. R., & Schacter, D. L. (2008). The brain's default network: anatomy, function, and relevance to disease. *Annals of the New York Academy of Sciences*, *1124*, 1–38.

Buckner, R. L., Krienen, F. M., Castellanos, A., Diaz, J. C., & Yeo, B. T. (2011). The organization of the human cerebellum estimated by intrinsic functional connectivity. *Journal of Neurophysiology*, *106*, 2322–2345.

Callisaya, M. L., Beare, R., Moran, C., Phan, T., Wang, W., & Srikanth, V. K. (2019). Type 2 diabetes mellitus, brain atrophy and cognitive decline in older people: A longitudinal study. *Diabetologia*, *62*(3), 448–458.

Cao, C., Liu, W., Zhang, Q., Wu, J.-l., Sun, Y., Li, D., … Wang, F. (2019). Irregular structural networks of gray matter in patients with type 2 diabetes mellitus. *Brain Imaging and Behavior*, *14*, 1477–1486.

Chen, X., Zhang, H., Gao, Y., Wee, C. Y., Li, G., Shen, D., & Alzheimer's Disease Neuroimaging Initiative. (2016). High-order resting-state functional connectivity network for MCI classification. *Human Brain Mapping*, *37*(9), 3282–3296.

Chen, X., Zhang, H., Lee, S.-W., Shen, D., & Alzheimer's Disease Neuroimaging Initiative. (2017). Hierarchical high-order functional connectivity networks and selective feature fusion for MCI classification. *Neuroinformatics*, *15*(3), 271–284.

Chen, X., Zhang, H., & Shen, D. (2016). Ensemble hierarchical high-order functional connectivity networks for MCI classification. Paper presented at the International Conference on Medical Image Computing and Computer-Assisted Intervention.

Chen, X., Zhang, H., Zhang, L., Shen, C., Lee, S. W., & Shen, D. (2017). Extraction of dynamic functional connectivity from brain grey matter and white matter for MCI classification. *Human Brain Mapping*, *38*(10), 5019–5034.

Chen, Y., Chen, K., Zhang, J., Li, X., Shu, N., Wang, J., … Reiman, E. M. (2015). Disrupted functional and structural networks in cognitively normal elderly subjects with the APOE ϵ4 allele. *Neuropsychopharmacology*, *40*(5), 1181–1191.

Chen, Y., Liu, Z., Zhang, J., Tian, G., Li, L., Zhang, S., … Zhang, Z. (2015). Selectively disrupted functional connectivity networks in type 2 diabetes mellitus. *Frontiers in Aging Neuroscience*, *7*, 233.

Chen, Y.-C., Jiao, Y., Cui, Y., Shang, S.-A., Ding, J., Feng, Y., … Teng, G.-J. (2014). Aberrant brain functional connectivity related to insulin resistance in type 2 diabetes: A resting-state fMRI study. *Diabetes Care*, *37*(6), 1689–1696.

Cheng, B., Liu, M., Zhang, D., Munsell, B. C., & Shen, D. (2015). Domain transfer learning for MCI conversion prediction. *IEEE Transactions on Biomedical Engineering*, *62*(7), 1805–1817.

Cheng, G., Huang, C., Deng, H., & Wang, H. (2012). Diabetes as a risk factor for dementia and mild cognitive impairment: A meta-analysis of longitudinal studies. *Internal Medicine Journal*, *42*(5), 484–491.

Corbetta, M., Kincade, J. M., & Shulman, G. L. (2002). Neural systems for visual orienting and their relationships to spatial working memory. *Journal of Cognitive Neuroscience*, *14*(3), 508–523.

Cortes, C., & Vapnik, V. (1995). Support-vector networks. *Machine Learning*, *20*(3), 273–297.

Cui, Y., Jiao, Y., Chen, H.-J., Ding, J., Luo, B., Peng, C.-Y., … Teng, G.-J. (2015). Aberrant functional connectivity of default-mode network in type 2 diabetes patients. *European Radiology*, *25*(11), 3238–3246.

Cui, Y., Jiao, Y., Chen, Y.-C., Wang, K., Gao, B., Wen, S., … Teng, G.-J. (2014). Altered spontaneous brain activity in type 2 diabetes: A resting-state functional MRI study. *Diabetes*, *63*(2), 749–760.

Dai, Z., Yan, C., Li, K., Wang, Z., Wang, J., Cao, M., … Bi, Y. (2015). Identifying and mapping connectivity patterns of brain network hubs in Alzheimer's disease. *Cerebral Cortex*, *25*(10), 3723–3742.

den Heijer, T., Vermeer, S., Van Dijk, E., Prins, N., Koudstaal, P., Hofman, A., & Breteler, M. (2003). Type 2 diabetes and atrophy of medial temporal lobe structures on brain MRI. *Diabetologia*, *46*(12), 1604–1610.

Dore, G. A., Elias, M. F., Robbins, M. A., Elias, P. K., & Nagy, Z. (2009). Presence of the APOE ε4 allele modifies the relationship between type 2 diabetes and cognitive performance: The Maine–Syracuse study. *Diabetologia*, *52*(12), 2551–2560.

El-Baz, A. H., Hassanien, A. E., & Schaefer, G. (2016). Identification of diabetes disease using committees of neural network-based classifiers. In *Machine intelligence and big data in industry* (pp. 65–74). Cham, Switzerland: Springer.

Elkayam, I., Ravona-Springer, R., Lin, H., Liu, X., Heymann, A., Melamed, Y., … Beeri, M. S. (2019). P1-248: A poorer level and more rapid decline in motor function in older adults with type 2 diabetes is associated with more rapid cognitive decline. *Alzheimer's & Dementia*, *15*, P334.

Exalto, L., Whitmer, R., Kappele, L., & Biessels, G. (2012). An update on type 2 diabetes, vascular dementia and Alzheimer's disease. *Experimental Gerontology*, *47*(11), 858–864.

Fan, Y., Rao, H., Hurt, H., Giannetta, J., Korczykowski, M., Shera, D., … Shen, D. (2007). Multivariate examination of brain abnormality using both structural and functional MRI. *NeuroImage*, *36*(4), 1189–1199.

Feinkohl, I., Price, J. F., Strachan, M. W., & Frier, B. M. (2015). The impact of diabetes on cognitive decline: Potential vascular, metabolic, and psychosocial risk factors. *Alzheimer's Research & Therapy*, *7*(1), 1–22.

Ferri, F., Frassinetti, F., Ardizzi, M., Costantini, M., & Gallese, V. (2012). A sensorimotor network for the bodily self. *Journal of Cognitive Neuroscience*, *24*(7), 1584–1595.

Fox, M. D., Corbetta, M., Snyder, A. Z., Vincent, J. L., & Raichle, M. E. (2006). Spontaneous neuronal activity distinguishes human dorsal and ventral attention systems. *Proceedings of the National Academy of Sciences*, *103*(26), 10046–10051.

Friston, K. J., Williams, S., Howard, R., Frackowiak, R. S., & Turner, R. (1996). Movement-related effects in fMRI time-series. *Magnetic Resonance in Medicine*, *35*(3), 346–355.

Garcia-Casares, N., Jorge, R. E., Garcia-Arnes, J. A., Acion, L., Berthier, M. L., Gonzalez-Alegre, P., … Rioja, J. (2014). Cognitive dysfunctions in middle-aged type 2 diabetic patients and neuroimaging correlations: A cross-sectional study. *Journal of Alzheimer's Disease*, *42*(4), 1337–1346.

Geijselaers, S. L., Sep, S. J., Stehouwer, C. D., & Biessels, G. J. (2015). Glucose regulation, cognition, and brain MRI in type 2 diabetes: A systematic review. *The Lancet Diabetes & Endocrinology*, *3*(1), 75–89.

Ghasemi, R., Haeri, A., Dargahi, L., Mohamed, Z., & Ahmadiani, A. (2013). Insulin in the brain: Sources, localization and functions. *Molecular Neurobiology*, *47*(1), 145–171.

Gong, Y. (1992). *Wechsler adult intelligence scale-revised in China version*. Changsha, Hunan/China: Hunan Medical College.

Gorniak, S. L., Ray, H., Lee, B.-C., & Wang, J. (2020). Cognitive–motor impairment in manual tasks in adults with type 2 diabetes. *Occupation, Participation and Health*, *40*(2), 113–121.

Gregg, E. W., Yaffe, K., Cauley, J. A., Rolka, D. B., Blackwell, T. L., Narayan, K. V., & Cummings, S. R. (2000). Is diabetes associated with cognitive impairment and cognitive decline among older women? *Archives of Internal Medicine*, *160*(2), 174–180.

Groeneveld, O. N., van den Berg, E., Johansen, O. E., Schnaidt, S., Hermansson, K., Zinman, B., … Biessels, G. J. (2019). Oxidative stress and endothelial dysfunction are associated with reduced cognition in type 2 diabetes. *Diabetes and Vascular Disease Research*, *16*(6), 577–581.

Hugenschmidt, C. E., Lovato, J. F., Ambrosius, W. T., Bryan, R. N., Gerstein, H. C., Horowitz, K. R., … Chew, E. Y. (2014). The cross-sectional and longitudinal associations of diabetic retinopathy with cognitive function and brain MRI findings: The action to control cardiovascular risk in diabetes (ACCORD) trial. *Diabetes Care*, *37*(12), 3244–3252.

Ip, H. H., & Shen, D. (1998). An affine-invariant active contour model (AI-snake) for model-based segmentation. *Image and Vision Computing*, *16*(2), 135–146.

Jia, H., Wu, G., Wang, Q., & Shen, D. (2010). ABSORB: Atlas building by self-organized registration and bundling. *NeuroImage*, *51*(3), 1057–1070.

Jia, H., Yap, P.-T., & Shen, D. (2012). Iterative multi-atlas-based multi-image segmentation with tree-based registration. *NeuroImage*, *59*(1), 422–430.

Kakrani, A., Gokhale, V., Vohra, K. V., & Chaudhary, N. (2014). Clinical and nerve conduction study correlation in patients of diabetic neuropathy. *The Journal of the Association of Physicians of India*, *62*(1), 24–27.

Kanaya, A. M., Barrett-Connor, E., Gildengorin, G., & Yaffe, K. (2004). Change in cognitive function by glucose tolerance status in older adults: A 4-year prospective study of the Rancho Bernardo study cohort. *Archives of Internal Medicine*, *164*(12), 1327–1333.

Li, Y., Liang, Y., Tan, X., Chen, Y., Yang, J., Zeng, H., … Qiu, S. (2020). Altered functional hubs and connectivity in type 2 diabetes mellitus without mild cognitive impairment. *Frontiers in Neurology*, *11*, 1016.

Liu, D., Duan, S., Zhang, J., Zhou, C., Liang, M., Yin, X., … Wang, J. (2016). Aberrant brain regional homogeneity and functional connectivity in middle-aged T2DM patients: A resting-state functional MRI study. *Frontiers in Human Neuroscience*, *10*, 490.

Liu, L., Zhang, H., Wu, J., Yu, Z., Chen, X., Rekik, I., … Shen, D. (2019). Overall survival time prediction for high-grade glioma patients based on large-scale brain functional networks. *Brain Imaging and Behavior*, *13*(5), 1333–1351.

Liu, Y., Liang, P., Duan, Y., Jia, X., Wang, F., Yu, C., … Li, K. (2011). Abnormal baseline brain activity in patients with neuromyelitis optica: A resting-state fMRI study. *European Journal of Radiology*, *80*(2), 407–411.

Luo, C., Chen, Q., Huang, R., Chen, X., Chen, K., Huang, X., … Shang, H.-F. (2012). Patterns of spontaneous brain activity in amyotrophic lateral sclerosis: A resting-state FMRI study. *PLoS One*, *7*(9), e45470.

Manschot, S. M., Brands, A. M., van der Grond, J., Kessels, R. P., Algra, A., Kappelle, L. J., & Biessels, G. J. (2006). Brain magnetic resonance imaging correlates of impaired cognition in patients with type 2 diabetes. *Diabetes*, *55*(4), 1106–1113.

Marek, S., Hwang, K., Foran, W., Hallquist, M. N., & Luna, B. (2015). The contribution of network organization and integration to the development of cognitive control. *PLoS Biology*, *13*(12), e1002328.

Marseglia, A., Fratiglioni, L., Laukka, E. J., Santoni, G., Pedersen, N. L., Bäckman, L., & Xu, W. (2016). Early cognitive deficits in type 2 diabetes: A population-based study. *Journal of Alzheimer's Disease*, *53*(3), 1069–1078.

Mattingley, J. B., Husain, M., Rorden, C., Kennard, C., & Driver, J. (1998). Motor role of human inferior parietal lobe revealed in unilateral neglect patients. *Nature*, *392*(6672), 179–182.

Mechelli, A., Humphreys, G. W., Mayall, K., Olson, A., & Price, C. J. (2000). Differential effects of word length and visual contrast in the fusiform and lingual gyri during. *Proceedings of the Royal Society of London, Series B: Biological Sciences*, *267*(1455), 1909–1913.

Meneilly, G. S., & Tessier, D. M. (2016). Diabetes, dementia and hypoglycemia. *Canadian Journal of Diabetes*, *40*(1), 73–76.

Messier, C. (2005). Impact of impaired glucose tolerance and type 2 diabetes on cognitive aging. *Neurobiology of Aging*, *26*(1), 26–30.

Misaki, M., Kim, Y., Bandettini, P. A., & Kriegeskorte, N. (2010). Comparison of multivariate classifiers and response normalizations for pattern-information fMRI. *NeuroImage*, *53*(1), 103–118.

Moheet, A., Mangia, S., & Seaquist, E. R. (2015). Impact of diabetes on cognitive function and brain structure. *Annals of the New York Academy of Sciences*, *1353*, 60–71.

Moran, C., Phan, T. G., Chen, J., Blizzard, L., Beare, R., Venn, A., … Greenaway, T. M. (2013). Brain atrophy in type 2 diabetes: Regional distribution and influence on cognition. *Diabetes Care*, *36*(12), 4036–4042.

Musen, G., Jacobson, A. M., Bolo, N. R., Simonson, D. C., Shenton, M. E., McCartney, R. L., … Hoogenboom, W. S. (2012). Resting-state brain functional connectivity is altered in type 2 diabetes. *Diabetes*, *61*(9), 2375–2379.

Nasreddine, Z. S., Phillips, N. A., Bédirian, V., Charbonneau, S., Whitehead, V., Collin, I., … Chertkow, H. (2005). The Montreal Cognitive Assessment, MoCA: A brief screening tool for mild cognitive impairment. *Journal of the American Geriatrics Society*, *53*(4), 695–699.

Nielsen, J. D., Madsen, K. H., Wang, Z., Liu, Z., Friston, K. J., & Zhou, Y. (2017). Working memory modulation of frontoparietal network connectivity in first-episode schizophrenia. *Cerebral Cortex*, *27*(7), 3832–3841.

Patton, N., Aslam, T., MacGillivray, T., Pattie, A., Deary, I. J., & Dhillon, B. (2005). Retinal vascular image analysis as a potential screening tool for cerebrovascular disease: A rationale based on homology between cerebral and retinal microvasculatures. *Journal of Anatomy*, *206*(4), 319–348.

Peng, J., Qu, H., Peng, J., Luo, T.-Y., Lv, F.-J., Wang, Z.-N., … Cheng, Q.-F. (2016). Abnormal spontaneous brain activity in type 2 diabetes with and without microangiopathy revealed by regional homogeneity. *European Journal of Radiology*, *85*(3), 607–615.

Power, J. D., Barnes, K. A., Snyder, A. Z., Schlaggar, B. L., & Petersen, S. E. (2012). Spurious but systematic correlations in functional connectivity MRI networks arise from subject motion. *NeuroImage*, *59*(3), 2142–2154.

Power, J. D., Mitra, A., Laumann, T. O., Snyder, A. Z., Schlaggar, B. L., & Petersen, S. E. (2014). Methods to detect, characterize, and remove motion artifact in resting state fMRI. *NeuroImage*, *84*, 320–341.

Power, J. D., Schlaggar, B. L., Lessov-Schlaggar, C. N., & Petersen, S. E. (2013). Evidence for hubs in human functional brain networks. *Neuron*, *79*(4), 798–813.

Preti, M. G., Bolton, T. A., & Van De Ville, D. (2017). The dynamic functional connectome: State-of-the-art and perspectives. *NeuroImage*, *160*, 41–54.

Redondo, M. T., Beltrán-Brotóns, J. L., Reales, J. M., & Ballesteros, S. (2016). Executive functions in patients with Alzheimer's disease, type 2 diabetes mellitus patients and cognitively healthy older adults. *Experimental Gerontology*, *83*, 47–55.

Russ, M. O., Mack, W., Grama, C.-R., Lanfermann, H., & Knopf, M. (2003). Enactment effect in memory: Evidence concerning the function of the supramarginal gyrus. *Experimental Brain Research*, *149*(4), 497–504.

Ryan, C. M., & Geckle, M. O. (2000). Circumscribed cognitive dysfunction in middle-aged adults with type 2 diabetes. *Diabetes Care*, *23*(10), 1486–1493.

Saedi, E., Gheini, M. R., Faiz, F., & Arami, M. A. (2016). Diabetes mellitus and cognitive impairments. *World Journal of Diabetes*, *7*(17), 412–422.

Samton, J. B., Ferrando, S. J., Sanelli, P., Karimi, S., Raiteri, V., & Barnhill, J. W. (2005). The clock drawing test: Diagnostic, functional, and neuroimaging correlates in older medically ill adults. *The Journal of Neuropsychiatry and Clinical Neurosciences*, *17*(4), 533–540.

Schmidt, M. (1996). *Rey auditory verbal learning test: A handbook*. CA: Western Psychological Services Los Angeles.

Schmidt, R., Launer, L. J., Nilsson, L.-G., Pajak, A., Sans, S., Berger, K., … Fuhrer, R. (2004). Magnetic resonance imaging of the brain in diabetes: The Cardiovascular Determinants of Dementia (CASCADE) Study. *Diabetes*, *53*(3), 687–692.

Sestieri, C., Corbetta, M., Romani, G. L., & Shulman, G. L. (2011). Episodic memory retrieval, parietal cortex, and the default mode network: Functional and topographic analyses. *Journal of Neuroscience*, *31*(12), 4407–4420.

Shu, N., Liang, Y., Li, H., Zhang, J., Li, X., Wang, L., … Zhang, Z. (2012). Disrupted topological organization in white matter structural networks in amnestic mild cognitive impairment: Relationship to subtype. *Radiology*, *265*(2), 518–527.

Singh, S., Kumar, M., Modi, S., Kaur, P., Shankar, L., & Khushu, S. (2015). Alterations of functional connectivity among resting-state networks in hypothyroidism. *Journal of Neuroendocrinology*, *27*(7), 609–615.

Sokolova, M., Japkowicz, N., & Szpakowicz, S. (2006). Beyond accuracy, F-score and ROC: a family of discriminant measures for performance evaluation. Paper presented at the Australasian joint conference on artificial intelligence.

Tibshirani, R. (1996). Regression shrinkage and selection via the lasso. *Journal of the Royal Statistical Society: Series B (Methodological)*, *58*(1), 267–288.

Tzourio-Mazoyer, N., Landeau, B., Papathanassiou, D., Crivello, F., Etard, O., Delcroix, N., … Joliot, M. (2002). Automated anatomical labeling of activations in SPM using a macroscopic anatomical parcellation of the MNI MRI single-subject brain. *NeuroImage*, *15*(1), 273–289.

Uddin, L. Q., Clare Kelly, A., Biswal, B. B., Xavier Castellanos, F., & Milham, M. P. (2009). Functional connectivity of default mode network components: Correlation, anticorrelation, and causality. *Human Brain Mapping*, *30*(2), 625–637.

Verdile, G., Fuller, S. J., & Martins, R. N. (2015). The role of type 2 diabetes in neurodegeneration. *Neurobiology of Disease*, *84*, 22–38.

Vincent, C., & Hall, P. A. (2015). Executive function in adults with type 2 diabetes: A meta-analytic review. *Psychosomatic Medicine*, *77*(6), 631–642.

Wang, C.-X., Fu, K.-L., Liu, H.-J., Xing, F., & Zhang, S.-Y. (2014). Spontaneous brain activity in type 2 diabetics revealed by amplitude of low-frequency fluctuations and its association with diabetic vascular disease: A resting-state FMRI study. *PLoS One*, *9*(10), e108883.

Wang, L., Li, H., Liang, Y., Zhang, J., Li, X., Shu, N., … Zhang, Z. (2013). Amnestic mild cognitive impairment: Topological reorganization of the default-mode network. *Radiology*, *268*(2), 501–514.

Wang, Z.-L., Zou, L., Lu, Z.-W., Xie, X.-Q., Jia, Z.-Z., Pan, C.-J., … Ge, X.-M. (2017). Abnormal spontaneous brain activity in type 2 diabetic retinopathy revealed by amplitude of low-frequency fluctuations: A resting-state fMRI study. *Clinical Radiology*, *72*(4), 340.e1–340.e7.

Whitwell, J. L., Josephs, K. A., Avula, R., Tosakulwong, N., Weigand, S., Senjem, M., … Baker, M. (2011). Altered functional connectivity in asymptomatic MAPT subjects: A comparison to bvFTD. *Neurology*, *77*(9), 866–874.

Wilson, G., Bryan, J., Cranston, K., Kitzes, J., Nederbragt, L., & Teal, T. K. (2017). Good enough practices in scientific computing. *PLoS Computational Biology*, *13*(6), e1005510.

Wood, A. G., Chen, J., Moran, C., Phan, T., Beare, R., Cooper, K., … Srikanth, V. (2016). Brain activation during memory encoding in type 2 diabetes mellitus: A discordant twin pair study. *Journal of Diabetes Research*, *2016*, 1–10.

Wu, G., Jia, H., Wang, Q., & Shen, D. (2011). SharpMean: Groupwise registration guided by sharp mean image and tree-based registration. *NeuroImage*, *56*(4), 1968–1981.

Xia, W., Wang, S., Rao, H., Spaeth, A. M., Wang, P., Yang, Y., … Sun, H. (2015). Disrupted resting-state attentional networks in T2DM patients. *Scientific Reports*, *5*, 11148.

Xia, W., Wang, S., Sun, Z., Bai, F., Zhou, Y., Yang, Y., … Yuan, Y. (2013). Altered baseline brain activity in type 2 diabetes: A resting-state fMRI study. *Psychoneuroendocrinology*, *38*(11), 2493–2501.

Yang, S.-Q., Xu, Z.-P., Xiong, Y., Zhan, Y.-F., Guo, L.-Y., Zhang, S., … Wang, J.-Z. (2016). Altered intranetwork and internetwork functional connectivity in type 2 diabetes mellitus with and without cognitive impairment. *Scientific Reports*, *6*, 32980.

Yeo, B. T., Krienen, F. M., Sepulcre, J., Sabuncu, M. R., Lashkari, D., Hollinshead, M., … Polimeni, J. R. (2011). The organization of the human cerebral cortex estimated by intrinsic functional connectivity. *Journal of Neurophysiology*, *106*(3), 1125–1165.

Yue, C., Xin, L., Kewen, X., & Chang, S. (2008). *An intelligent diagnosis to type 2 diabetes based on QPSO algorithm and WLS-SVM*. Paper presented at the 2008 International Symposium on Intelligent Information Technology Application Workshops.

Zeng, L.-L., Shen, H., Liu, L., Wang, L., Li, B., Fang, P., … Hu, D. (2012). Identifying major depression using whole-brain functional connectivity: A multivariate pattern analysis. *Brain*, *135*(5), 1498–1507.

Zhang, H., Chen, X., Zhang, Y., & Shen, D. (2017). Test-retest reliability of "high-order" functional connectivity in young healthy adults. *Frontiers in Neuroscience*, *11*, 439.

Zhang, H., Hao, Y., Manor, B., Novak, P., Milberg, W., Zhang, J., … Novak, V. (2015). Intranasal insulin enhanced resting-state functional connectivity of hippocampal regions in type 2 diabetes. *Diabetes*, *64*(3), 1025–1034.

Zhang, L. J., Zheng, G., Zhang, L., Zhong, J., Li, Q., Zhao, T. Z., & Lu, G. M. (2014). Disrupted small world networks in patients without overt hepatic encephalopathy: A resting state fMRI study. *European Journal of Radiology*, *83*(10), 1890–1899.

Zhang, Y., Zhang, H., Chen, X., Liu, M., Zhu, X., Lee, S.-W., & Shen, D. (2019). Strength and similarity guided group-level brain functional network construction for MCI diagnosis. *Pattern Recognition*, *88*, 421–430.

Zheng, Y., Chen, X., Li, D., Liu, Y., Tan, X., Liang, Y., … Shen, D. (2019). Treatment-naïve first episode depression classification based on high-order brain functional network. *Journal of Affective Disorders*, *256*, 33–41.

Zhou, H., Lu, W., Shi, Y., Bai, F., Chang, J., Yuan, Y., … Zhang, Z. (2010). Impairments in cognition and resting-state connectivity of the hippocampus in elderly subjects with type 2 diabetes. *Neuroscience Letters*, *473*(1), 5–10.

Zhou, Z., Chen, X., Zhang, Y., Hu, D., Qiao, L., Yu, R., … Shen, D. (2020). A toolbox for brain network construction and classification (BrainNetClass). *Human Brain Mapping*, *41*(10), 2808–2826.

Zhou, Z., Wang, J.-B., Zang, Y.-F., & Pan, G. (2018). PAIR comparison between two within-group conditions of resting-state fMRI improves classification accuracy. *Frontiers in Neuroscience*, *11*, 740.

SUPPORTING INFORMATION

Additional supporting information may be found online in the Supporting Information section at the end of this article.

How to cite this article: Chen, Y., Zhou, Z., Liang, Y., Tan, X., Li, Y., Qin, C., Feng, Y., Ma, X., Mo, Z., Xia, J., Zhang, H., Qiu, S., & Shen, D. (2021). Classification of type 2 diabetes mellitus with or without cognitive impairment from healthy controls using high-order functional connectivity. *Human Brain Mapping*, *42*(14), 4671–4684. https://doi.org/10.1002/hbm.25575